JOURNAL OF GUIDANCE, CONTROL, AND DYNAMICS
Vol. 27, No. 1, January–February 2004

Interspacecraft Optical Communication and Navigation Using Modulating Retroreflectors

N. Glenn Creamer,* G. Charmaine Gilbreath,† Timothy J. Meehan,‡ Michael J. Vilcheck,§
John A. Vasquez,¶ William S. Rabinovich,** and Peter G. Goetz††
U.S. Naval Research Laboratory, Washington, D.C. 20375
and
Rita Mahon‡‡
Jaycor, Inc., McLean, Virginia 22102

A novel concept is described for optical interrogation, communication, and navigation between pursuer and target spacecraft platforms. The technique uses a gimbaled laser source on the pursuer spacecraft and an array of eight solid-state, multiple quantum, well modulating retroreflectors on the target spacecraft. The sensor system provides high-bandwidth optical communication, centimeter-level relative positioning, and arc-minute-level relative orientation of the target platform with minimal sacrifice in target size, weight, and power. To accomplish the relative navigation, each target retroreflected signal is modulated with a unique code sequence, allowing for individual discrimination of the returned composite signal from a single photodetector on the pursuer platform. Experimental results using a dual-platform, multi-degree-of-freedom robotics testbed provide verification and demonstration of the concept, highlighting its potential for applications such as interspacecraft rendezvous and capture, long-baseline space interferometry, and formation flying.

I. Introduction

BECAUSE of the benefits of autonomous spacecraft-to-spacecraft interrogation, communication, and navigation for civilian, commercial, and military space missions, there has been a significant amount of research and development on associated relative sensor systems over the past few years.[1–8] These systems typically implement radio (rf) communication links, global positioning system (GPS) sensing for long-range relative positioning, and combinations of visual and laser ranging for short-range proximity operations. Most approaches require the target spacecraft to possess an rf antenna and transmitter along with a GPS sensor to transmit navigational data to the pursuer spacecraft. Additionally, any strategies requiring GPS availability are not suitable for geosynchronous or deep space missions unless a quasi-GPS system is emulated between each vehicle.[9] Although the visual/laser systems provide sufficient accuracy of relative states for close-in operations (that is, 0–50 m), their mid- to long-range capability (that is, >50 m) becomes significantly cruder, with relative position and attitude errors reaching tens of meters and tens of degrees at ranges exceeding 100 m.

In this paper, we develop and test a novel concept utilizing solid-state multiple quantum well (MQW) modulating retroreflectors to provide interspacecraft laser interrogation, communication, and navigation. The modulating retroreflectors enable compact, low-power, and low-mass optical data transfer on the order of megabits per second (Ref. 10) and relative navigation on the order of centimeters in three-axis position and arcminutes in two-axis orientation. Links over ranges of kilometers down to a few meters are possible. For close-proximity operations of about 10 m or less (docking missions, for example), this concept could work harmoniously with a vision-based system or possibly be utilized as a single-sensor solution with appropriate adaptable optics.

II. Multiple Quantum Well Modulating Retroreflectors

Modulating retroreflector (MRR) devices utilizing MQW technology provide a low-power, low-weight, multi-functional solution for the need to reduce parasitic payload requirements over conventional communications technologies. An MQW modulating retroreflector is a solid-state device that allows optical communication and ranging between two platforms. MQW shutters are particularly suited to these applications because the technology enables fast data rates, requires very low-drive powers, is lightweight, is robust, and is not polarization sensitive.[11,12] The device is also radiation hard.[§§]

Implementation of such devices requires that only one of the platforms have an onboard laser, telescope, and tracker. Thus, the device is well suited to asymmetric problems in which one platform has a large payload capacity and serves as the pursuer and interrogator and the other platform serves as a probe. As shown in Fig. 1, the pursuer illuminates the target platform carrying the MMRs with a laser beam. The laser beam is automatically reflected back to the pursuer, with no need for target pointing or tracking. The reflected return can be modulated in an on–off keying (OOK) mode using the MQW solid-state shutters.

The modulator must possess several characteristics to enable an efficient link. The shutter must have a high switching speed, low-power consumption, large area, wide field-of-view, and high optical quality. In addition, it must work at wavelengths where good laser sources are available and be radiation tolerant (for space applications) and rugged. Semiconductor multiple quantum well modulators are one of the few technologies that meet all of these requirements.[13,14] When a moderate voltage (on the order of 7–20 V) is placed across the device in reverse bias, the light absorption feature changes, both shifting in wavelength and changing in magnitude. Thus, the transmission of the device near this absorption feature changes dramatically and can serve as a solid-state on–off shutter.

Received 16 September 2002; revision received 19 June 2003; accepted for publication 23 June 2003.

*Aerospace Engineer, Code 8231, 4555 Overlook Avenue. Senior Member AIAA.
†Physicist, Code 7215, 4555 Overlook Avenue.
‡Electrical Engineer, Code 8121, 4555 Overlook Avenue.
§Electrical Engineer, Code 8123, 4555 Overlook Avenue.
¶Mechanical Engineer, Code 8222, 4555 Overlook Avenue.
**Physicist, Code 5654, 4555 Overlook Avenue.
††Physicist, Code 5652, 4555 Overlook Avenue.
‡‡Physicist.

[§§]Data available online at the U.S. Naval Research Laboratory's (NRL's) MRR web page at http://mrr.nrl.navy.mil [cited January 2001].

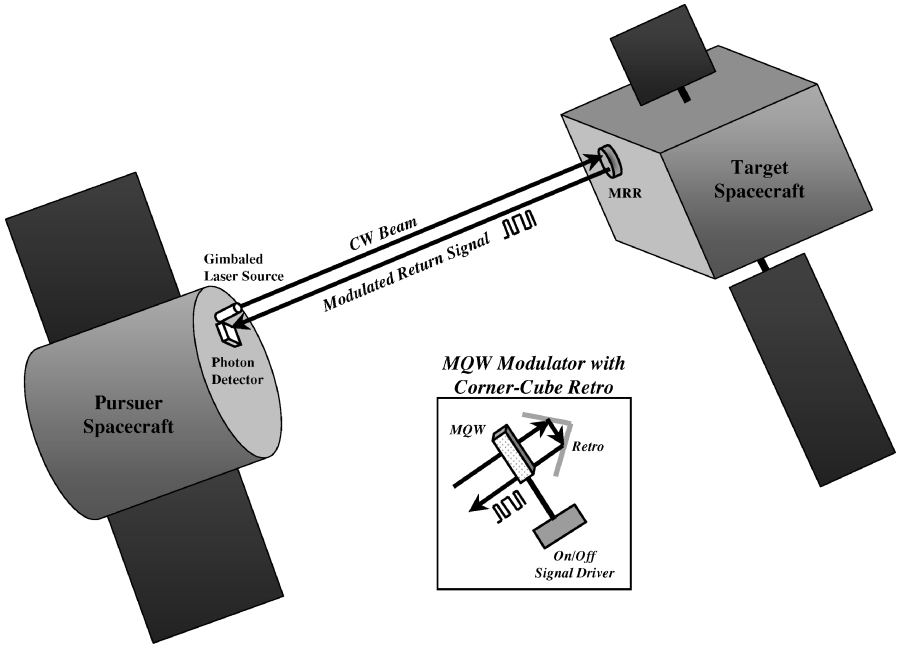

Fig. 1 Conceptual depiction of interspacecraft communication using modulating retroreflectors.

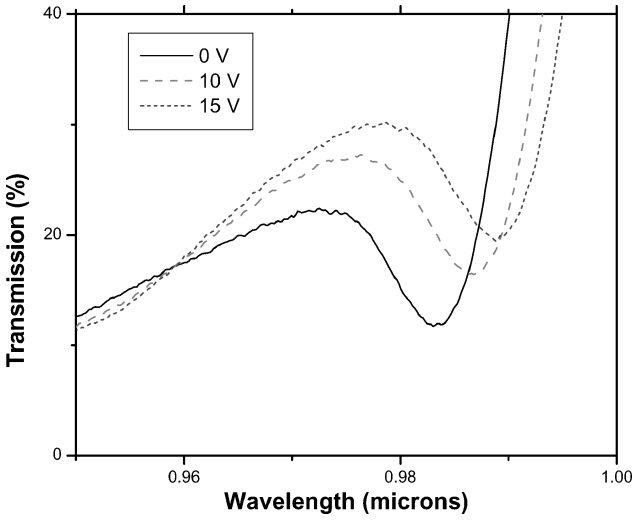

Fig. 2 Switching characteristics of an InGaAs-Based MQW modulator.

This switching capability is shown in Fig. 2 for an InGaAs-based MQW modulator. As shown in Fig. 2, the optical transmission level for the device changes as a function of drive voltage and wavelength, demonstrating a contrast ratio of 3 for a 980-nm device with a drive voltage of 15 V.

Unlike liquid crystal modulators, MQW modulators have very high switching speeds. Small devices (diameters in micrometers) have been operated at speeds in the tens of gigahertz. In practice, the speed is limited primarily by the resistance/capacitance time constant of the device. Thus, the large-area devices (on the order of a centimeter) used for retromodulator-based communications typically have speeds between 1 and 10 Mbps. Higher speeds are possible, however, depending on range and the sophistication of the fabrication process. For this effort, the devices were configured to operate at 1 Mbps.

In practice, the link (rather than the modulator) limits performance of an MRR system, except for close ranges. For a conventional corner-cube MRR, MQW technology should allow data rates in the tens of megabits per second, depending on the range and the interrogator system. For a diffraction-limited system, the optical

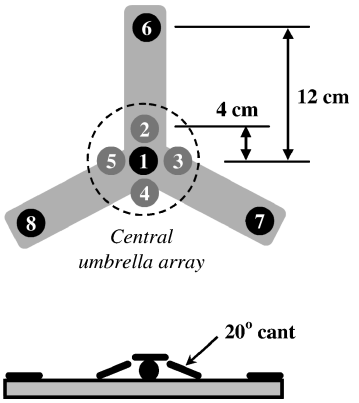

Fig. 3 Target MRR array.

power retroreflected from the target platform back to the pursuer platform scales as[15]

$$\frac{P_{\text{laser}} D_{\text{retro}}^4 D_{\text{rec}}^2}{\theta_{\text{div}}^2 \rho^4 \lambda^2} \tag{1}$$

where P_{laser} is the power of the laser transmitter, D_{retro} is the diameter of the target modulating retroreflector, D_{rec} is the diameter of the pursuer receive telescope, θ_{div} is the divergence of the transmitted laser beam, ρ is the range between the two platforms, and λ is the laser wavelength. The strongest dependencies are on the range and the corner-cube retromodulator diameter, both of which scale as fourth powers for diffraction-limited payloads. Retroreflector-based links fall off more strongly with range than conventional links because of their bidirectional nature.

III. Target Spacecraft MRR Array

To achieve relative three-axis positional tracking and two-axis orientation of the target platform, a target board was designed using a sensor array consisting of eight modulating retroreflectors, as shown in Fig. 3. The center retroreflector (MRR1) and outer three retroreflectors (MRR6, MRR7, and MRR8) lie in the same plane, and the four inner retroreflectors (MRR2, MRR3, MRR4, and MRR5) surrounding the center are canted 20 deg from the plane. On illumination of the entire array by the pursuer laser beam, the reflected signals from each MRR are uniquely modulated using MQW OOK

and returned to the pursuer. The intensity of each reflected signal is linearly proportional to the angle of the incoming laser beam relative to the MRR boresight, as shown in the test data of Fig. 4 for a typical retroreflector. This proportionality is exploited to determine the navigation solution. As described later, the signal intensities from the outer three retroreflectors are used for laser gimbal tracking control, and the signal intensities from the inner five retroreflectors are used to determine relative orientation.

IV. Pursuer Spacecraft Laser Interrogator, Detector, and Signal Processing Logic

The pursuer spacecraft houses the interrogating gimbaled laser, an analog photodetector, an analog-to-digital converter, and the associated signal processing logic required to transmit the continuous-wave laser beam to the target and to receive the reflected, modulated signals from the target MRR array. As shown in Fig. 5, the aggregate photon return is captured by the analog photodetector and converted to a digital signal through the analog-to-digital converter. Discrimination and isolation of each individual MRR signal is then achieved through a set of matching filters tuned to the unique modulator code sequence associated with each MRR. These eight isolated signals are then utilized to determine the relative navigation solution. Additionally, any critical target information can be easily transmitted to the pursuer by modulating the center MRR signal return with the data in binary on–off form.

V. Interspacecraft Relative Navigation Equations

To determine the target relative navigation solution, the pursuer's gimbaled laser is required to detect and track the MRR array as it moves in free space. Initial detection is achieved by performing a series of decreasing rectangular searches in gimbal azimuth and elevation space based on predefined signal threshold levels. As the laser beam crosses the MRR array, the return signal level will quickly increase until the threshold is reached, initiating a tighter search pattern. This iterative process is continued until a maximum signal level is obtained and all retroreflectors are illuminated. Subsequent gimbal tracking is achieved by equalizing the signal return intensities from the three outer retroreflectors on the target board, resulting in a laser beam that is continually centered on the MRR array.

The notational definitions for interspacecraft relative geometry are shown in Fig. 6. The relative position vector $\bar{\boldsymbol{R}}$ is determined from the range ρ and the laser beam unit vector $\boldsymbol{l}$, yielding

$$\bar{\boldsymbol{R}} = \rho \boldsymbol{l} = \rho(\cos EL \cos AZ \boldsymbol{p}_1 + \cos EL \sin AZ \boldsymbol{p}_2 + \sin EL \boldsymbol{p}_3) \tag{2}$$

where $\boldsymbol{p}_1$, $\boldsymbol{p}_2$, and $\boldsymbol{p}_3$ are orthogonal unit basis vectors defining the pursuer frame and AZ and EL are the gimbal azimuth and elevation angles, respectively, measured by the gimbal encoders relative to the pursuer frame. The range measurement to the central retroreflector is determined from time-of-flight (TOF) techniques, similar to the approach used by laser range finders for surveying. The TOF is obtained by measuring the round-trip time it takes a pulse to travel from the laser diode to the retroreflector and back, yielding

$$\rho = \tfrac{1}{2}(\mathrm{TOF} \times c) \tag{3}$$

where c is the speed of light.

The relative two-axis orientation matrix relating the target frame $\boldsymbol{T}$ to the pursuer frame $\boldsymbol{P}$ is determined using a 3–2 Euler angle sequence, yielding

$$C_{T/P} = \begin{bmatrix} \cos\theta & 0 & -\sin\theta \\ 0 & 1 & 0 \\ \sin\theta & 0 & \cos\theta \end{bmatrix} \begin{bmatrix} \cos\psi & \sin\psi & 0 \\ -\sin\psi & \cos\psi & 0 \\ 0 & 0 & 1 \end{bmatrix} \tag{4}$$

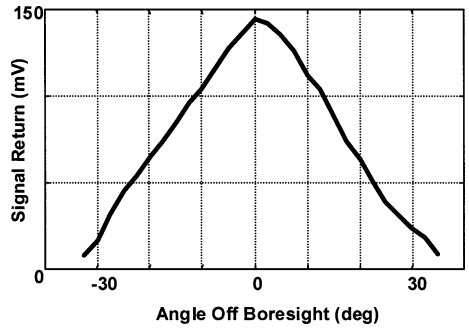

Fig. 4 Sensitivity of MRR signal intensity to off-boresight illumination.

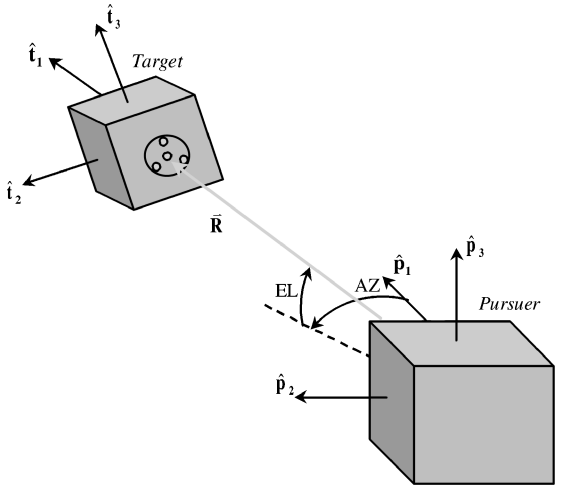

Fig. 6 Geometry for interspacecraft relative navigation.

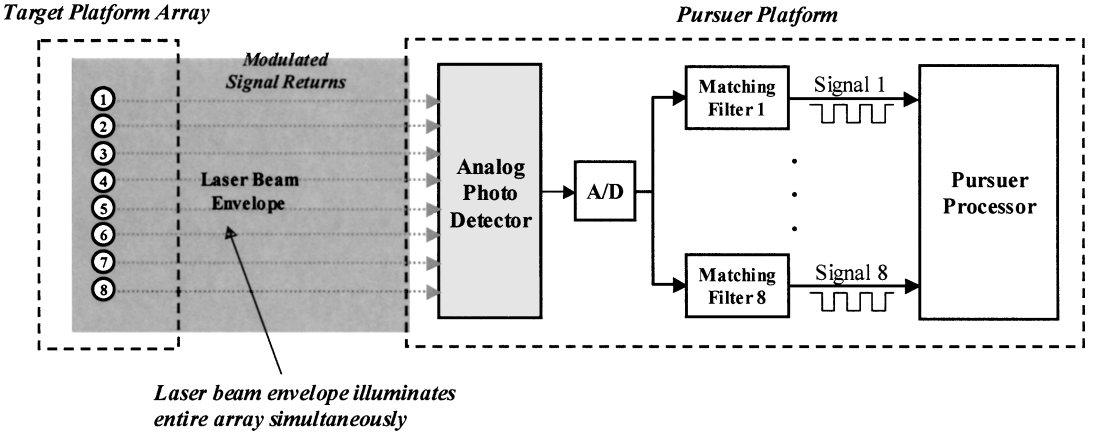

Fig. 5 Target-to-pursuer communication and MRR discrimination approach.

where ψ and θ are relative yaw and pitch aspect angles, respectively. The two aspect angles are derived from the relative signal intensities of each of the five central retroreflectors. For an incoming laser beam at an angle α_i relative to the ith MRR boresight, the reflected signal intensity becomes

$$S_i = S_0 - m\alpha_i \tag{5}$$

where S_0 is the maximum intensity return if the laser were directly on boresight and m is the slope of the straight line given in Fig. 4. When the numbering scheme from Fig. 3 is adopted, and yaw and pitch motion is uncoupled by assuming relatively small aspect angles (~30 deg or less), an estimate of these angles is as follows.

If $S_3 > S_5$:

$$\psi = AZ - \tfrac{1}{2}[(S_3 - S_5)/(S_1 - S_5)]\beta \tag{6a}$$

Else:

$$\psi = AZ + \tfrac{1}{2}[(S_5 - S_3)/(S_1 - S_3)]\beta \tag{6b}$$

If $S_2 > S_4$:

$$\theta = EL - \tfrac{1}{2}[(S_2 - S_4)/(S_1 - S_4)]\beta \tag{6c}$$

Else:

$$\theta = EL + \tfrac{1}{2}[(S_4 - S_2)/(S_1 - S_2)]\beta \tag{6d}$$

where β is the known cant angle of the four inner canted retroreflectors and it is assumed that the gimbal azimuth and elevation angles are also relatively small such that they are approximately aligned with the pursuer $\boldsymbol{p}_3$ and $\boldsymbol{p}_2$ axes, respectively. It is clear that this differencing strategy eliminates the need for experimentally calibrating the fixed bias S_0 and the slope m. Additionally, the intensity-based approach eliminates the need for tedious and precise clock synchronization that would be required of a TOF-based strategy in which the target orientation is estimated from the relative ranges to each MRR. Last, because the sensitivity of the signal return intensity is directly proportional to the angle off boresight, this strategy is, in principle, independent of range as long as sufficient laser power is available for long-range operations (tens of kilometers).

The five-state navigation solution derived from Eqs. (2–6) provides the relative position vector and aspect angles of the target platform. During illumination of the entire MRR array, the relative roll angle about the laser beam unit vector $\boldsymbol{l}$ is unobservable because the return signal intensities are insensitive to that angle. In the event of handover to a vision-based camera for close proximity operations such as target capture, this angle would be observable from the vision system after handover is completed. For other mission scenarios, this angle could either be deduced to some coarse level of accuracy from approximately known target dynamics (such as gravity-gradient stabilization) or estimated by traversing the laser beam across the array board and identifying the resulting signal drop-outs. For this effort, the relative roll angle is assumed to be negligible.

VI. Experimental Verification Using NRL's Dual-Platform Dynamic Motion Simulator

The NRL's dynamic motion simulator (DMS) was used for validation and performance evaluation of the interspacecraft MRR sensor system. As shown in the photograph of Fig. 7, the DMS facility consists of a six-degree-of-freedom pursuer platform and a four-degree-of-freedom target platform, each driven autonomously and independently using a Pentium III personal computer. The pursuer platform travels in the horizontal plane using an x–y trolley system and in the vertical direction, as well as in three rotational directions (yaw, pitch, and roll), using a robotic manipulator arm. The target platform travels in the horizontal plane using an x–y trolley system, as well as in two rotational directions (yaw and pitch), using a two-axis gimbal mechanism. The repeatable accuracy of the facility is a few millimeters in position and a fractions of an arcminute in rotation, valid over a workspace volume of about $30 \times 15 \times 3$ m.

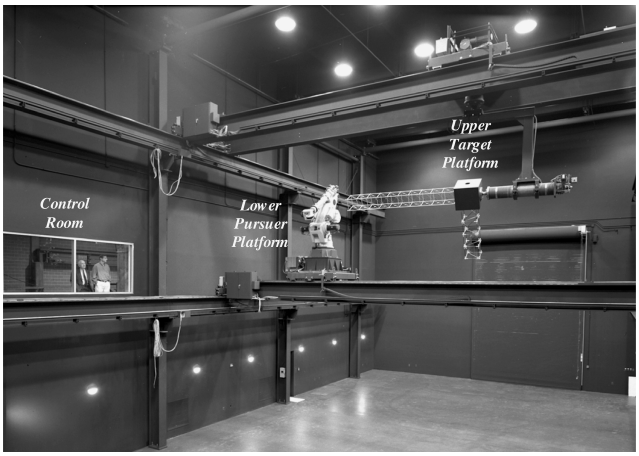

Fig. 7 NRL's dual-platform DMS.

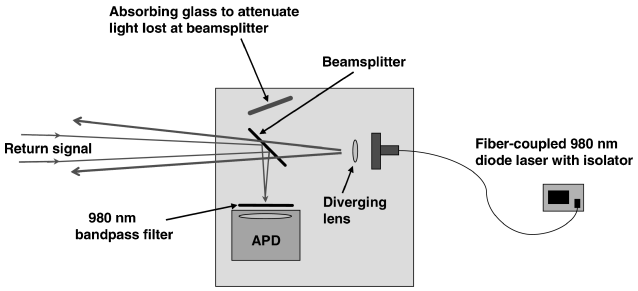

Fig. 8 Optical configuration used to illuminate target array and receive MRR signals.

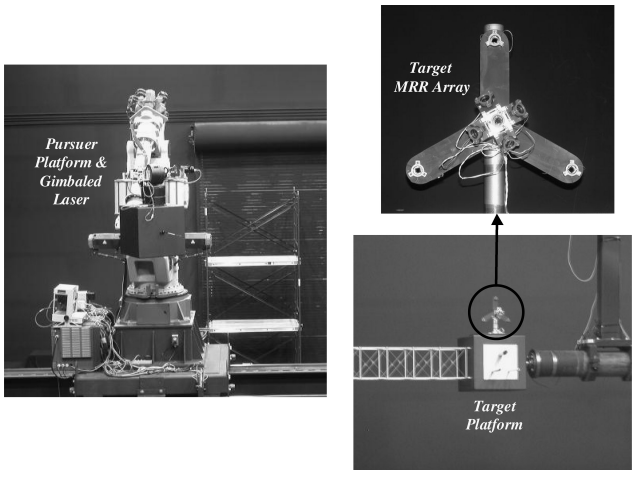

Fig. 9 Pursuer and target platform hardware.

The pursuer platform was equipped with a gimbaled optical transmitter/receiver system comprising a 100-mW laser diode operating at a 980-nm wavelength, a 10-MHz Avalanche Photodetector (APD), a signal amplifier, an analog-to-digital converter, and eight digital matched filters. The optical configuration, shown in Fig. 8, was monostatic and used a partially transmissive flat for aperture sharing. As can be seen from Fig. 8, the laser diode was fiber coupled to diverging optics that produced a 60-mrad beam. The retroreflected return was received and directed by the angled flat through a 980-nm-bandpass optical filter and focused onto the APD. Although the 60-mrad divergence was necessary for short-range operation, that is, meters, to illuminate the target board, a much smaller level of divergence would be utilized for long-range operation, that is, kilometers. This could be accomplished by selecting an appropriate diverging lens, based on target range, using a simple rotating wheel.

The target platform was equipped with the MRR array, consisting of eight 0.5-mm MQW MRRs. Each individual MRR has a mass

of about 10 g (including the holder) and draws about 75 mW of power. The units were driven with 15 V, sufficient to achieve 3:1 optical on–off modulation. Photographs of the hardware resident on the pursuer and target platforms are provided in Fig. 9.

Each target MRR was driven by a unique code that was detected, isolated, demodulated, and transformed into an intensity level for use by the acquisition and tracking logic. The eight codes used to modulate the MRR units are provided in Fig. 10. When a search-and-detect scanning profile was performed with the gimbaled laser system, the eight codes were detected and acquired. This search, detection, and acquisition profile is shown in Fig. 11, wherein the three outer MRR return intensities are equalized once lock-on of the entire array is achieved. The intensity levels from each MRR were then processed by the computer to determine the five-state relative navigation solution and subsequently activate simple proportional/derivative closed-loop control logic to perform both initial alignment to the target platform, as well as target tracking. A block diagram of the pursuer position and attitude controller is provided in Fig. 12. The pursuer rate and velocity feedback signals were derived from the motion of the platform rather than directly measured, though an actual spacecraft would likely utilize gyros and accelerometers to provide this information. Additionally, the current system does not include appropriate timing electronics necessary to determine accurate TOF ranging, and so range measurements were derived from the encoder information on each platform trolley system. Future facility upgrades will include the TOF ranging electronics.

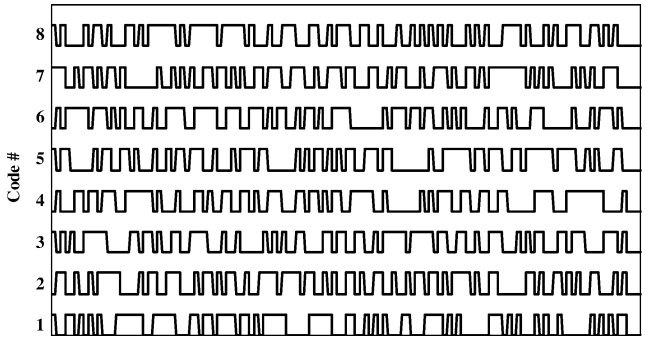

Fig. 10 Eight unique MRR code sequences.

As shown in Fig. 13, two closed-loop relative navigation and control tests were performed. The first test consisted of alignment of the pursuer platform frame to a stationary target frame with a commanded 10-m offset along the platform x axis. The second test consisted of a tracking maneuver in which the pursuer platform was commanded to maintain the 10-m offset and alignment to the target while the target moved along a circular 5-m radius arc in the horizontal plane. When a 30-deg arc was completed, the target then reversed direction and returned to its initial location.

Results from both maneuvers are provided in Figs. 14 and 15. In Figs. 14 and 15, the three-axis position error, the two-axis aspect error, and the two laser gimbal angles are provided. Note in Fig. 14, for the stationary target, that an initial position error of 9 m (primarily

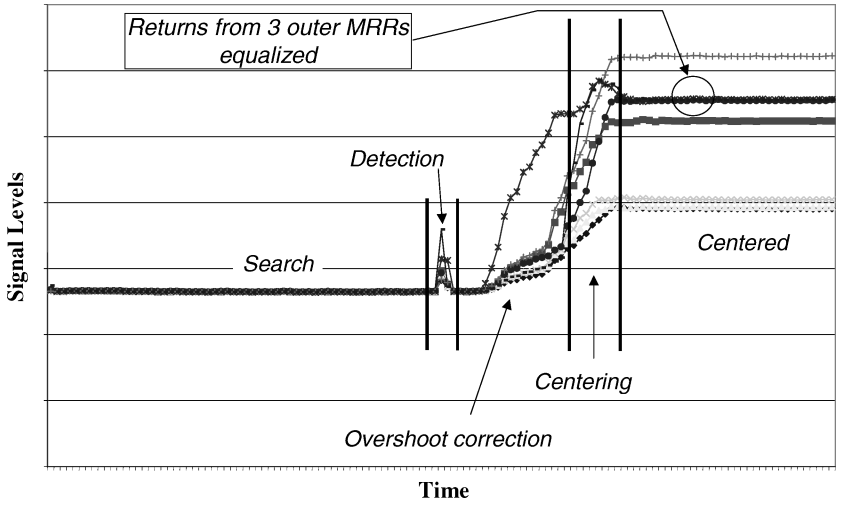

Fig. 11 Typical gimbaled laser search, detection, and acquisition of target MRR array.

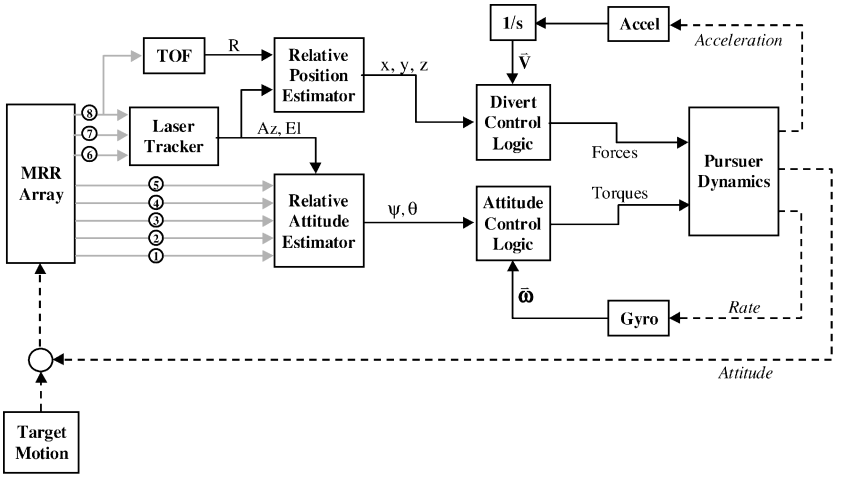

Fig. 12 Pursuer tracking control block diagram.

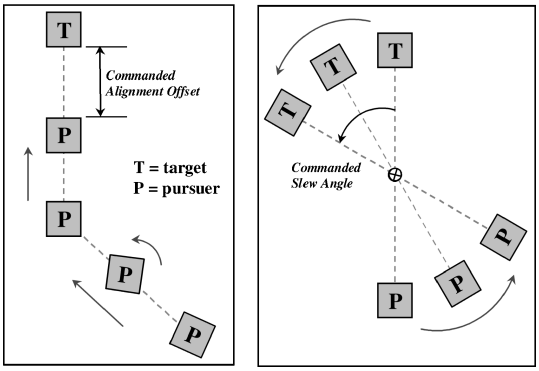

a) Alignment to Stationary target **b) Tracking moving target**

Fig. 13 Closed-loop tests used for concept verification and performance evaluation.

along the x axis) was removed within 6 min and an initial aspect error of 5 deg was removed within 2 min. In Fig. 15, note that small tracking errors occurred while the target was in motion (due to the low feedback control bandwidth of approximately 0.02 Hz), with the two large position error spikes due to target motion reversal and cessation. Of course, the steady-state tracking errors are highly dependent on the feedback control logic and gains selected for the tracking controller. For both tests, the steady-state 1-sigma tracking control errors were about 1 cm in position and 0.3 deg in orientation, due primarily to controller hardware limitations.

To obtain a quantitative measure of the sensor accuracy for measuring relative orientation of the target (in the absence of control errors), a static test was also performed in which the target and pursuer were aligned and held motionless. Figure 16 shows the resulting two-axis orientation error derived from the MRR signals, where it is observed that the sensor can potentially provide arcminute-level attitude knowledge.

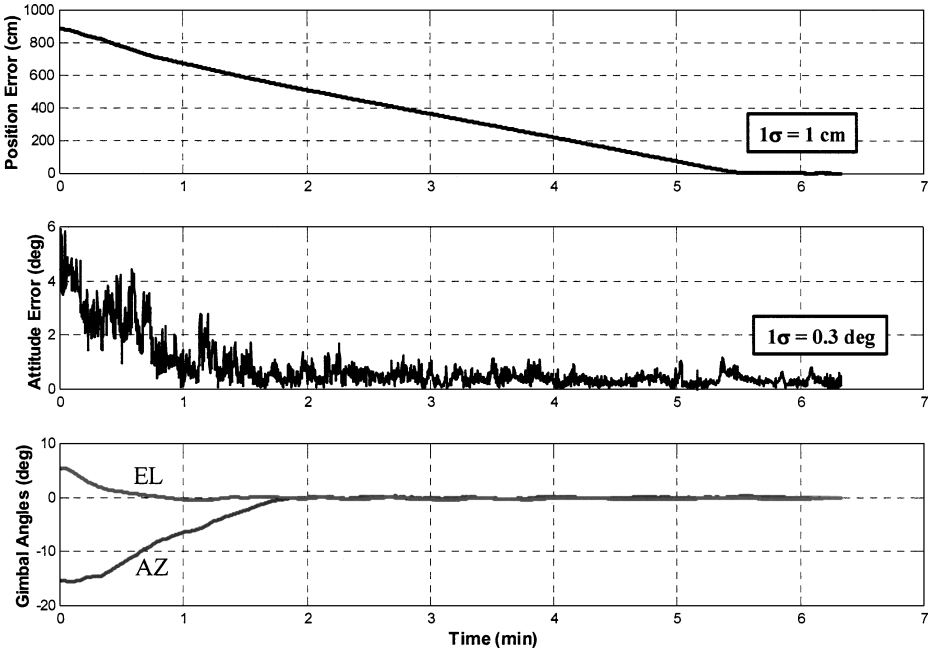

Fig. 14 Experimental results for alignment to a stationary target.

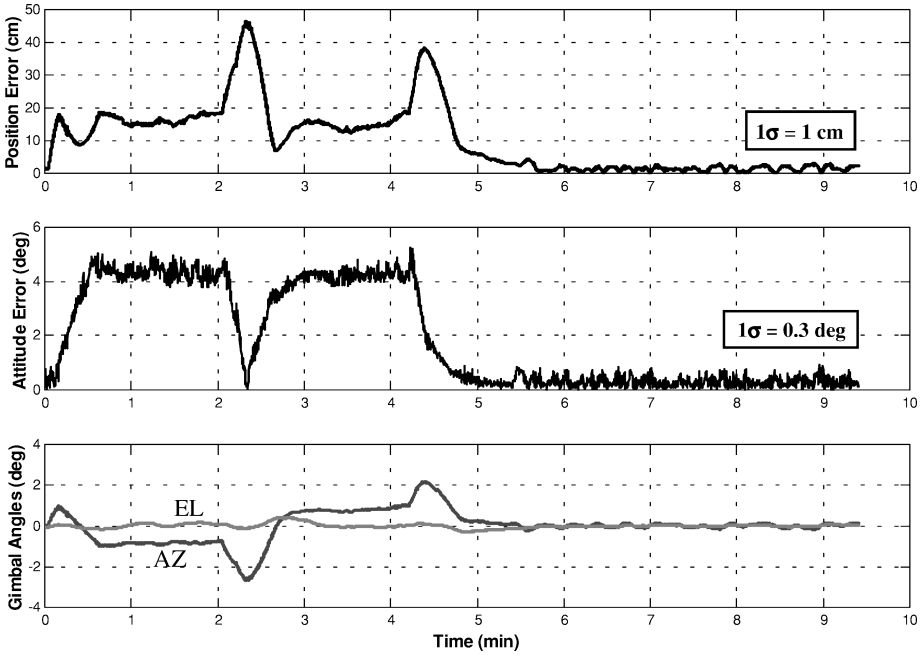

Fig. 15 Experimental results for tracking a moving target.

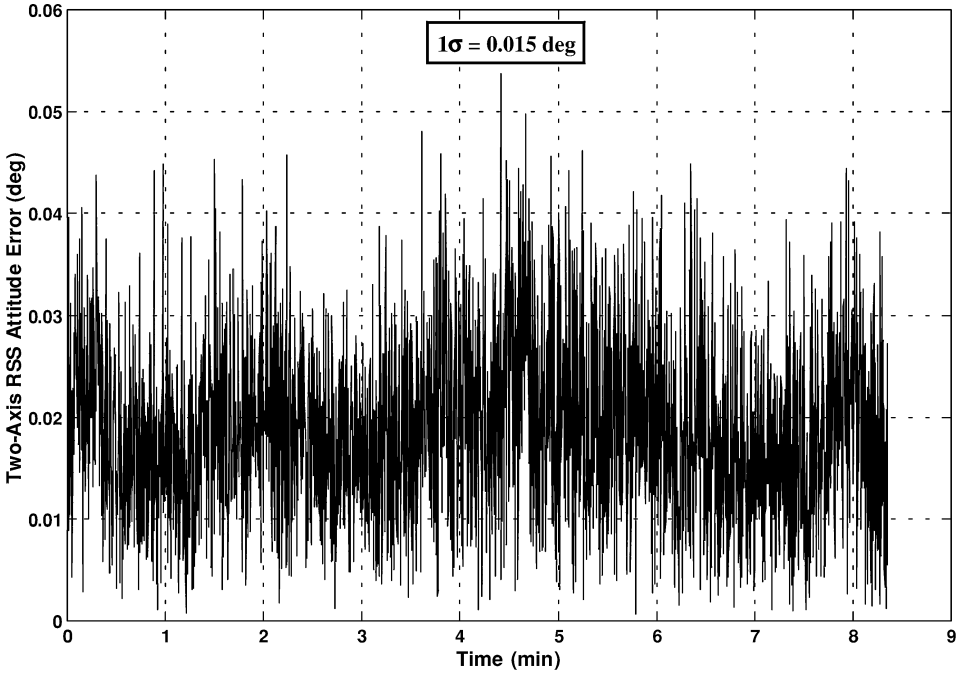

Fig. 16 Experimental results for static two-axis aspect estimation.

VII. Conclusions

We have designed, developed, and experimentally verified a novel dual-use sensor for simultaneous interspacecraft optical communication and navigation. The optical communication link from the target to the pursuer is established by illuminating a target platform with a laser beam from an interrogating pursuer platform. The beam illuminates an array of MMRs, which are uniquely coded to provide return signatures to the pursuer craft. The target's relative position vector and aspect angles are derived from the relative intensities of the modulated signal returns from each retroreflector on the target array. Signal discrimination is achieved by passing the aggregate photon return through a set of matching filters tuned to each unique retroreflector modulation code. Utilization of MQW corner-cube retroreflectors enables the target array to be populated with devices that require only milliwatts of power, are light and compact, and are radiation hard.

Experimental results using a dual-platform dynamic testbed have demonstrated and verified the concept. Initial alignment to a stationary target and alignment tracking and maintenance with respect to a moving target have been successfully demonstrated over a range of 10–20 m, though the concept is valid for ranges up to tens of kilometers provided sufficient laser power is available. The results show promise for applications such as autonomous rendezvous and capture, spacecraft formation flying, and free-flying space interferometry.

Acknowledgments

We are grateful to NASA Space Sciences for their support of this research project and to the reviewers for their constructive remarks.

References

[1]Polites, M. E., "Technology of Automated Rendezvous and Capture in Space," *Journal of Spacecraft and Rockets*, Vol. 36, No. 2, 1999, pp. 280–291.

[2]Junkins, J. L., Hughes, D., Wazni, K., and Pariyapong, V., "Vision-Based Navigation for Rendezvous, Docking, and Proximity Operations," *22nd Annual AAS Guidance and Control Conference*, American Astronautical Society, Breckenridge, CO, 1999, pp. 203–220.

[3]Mokuno, M., Kawano, I., and Kasai, T., "Experimental Results of Autonomous Rendezvous Docking on Japanese ETS-VII Satellite," *22nd Annual AAS Guidance and Control Conference*, American Astronautical Society, Breckenridge, CO, 1999, pp. 221–238.

[4]D'Souza, C., Bogner, A., and Brand, T., "An Evaluation of the GPS Relative Navigation System for ETS-VII and HTV," *22nd Annual AAS Guidance and Control Conference*, American Astronautical Society, Breckenridge, CO, 1999, pp. 239–258.

[5]Cislaghi, M., Fehse, W., Paris, D., and Ankerson, F., "The ATV Rendezvous Predevelopment Programme (ARP)," *22nd Annual AAS Guidance and Control Conference*, American Astronautical Society, Breckenridge, CO, 1999, pp. 259–280.

[6]Howard, R. T., Bryan, T. C., Book, M. L., and Dabney, R. W., "The Video Guidance Sensor—A Flight Proven Technology," *22nd Annual AAS Guidance and Control Conference*, American Astronautical Society, Breckenridge, CO, 1999, pp. 281–298.

[7]Cruzen, C. A., Lomas, J. J., and Dabney, R. W., "Test Results for the Automated Rendezvous and Capture System," *23nd Annual AAS Guidance and Control Conference*, American Astronautical Society, Breckenridge, CO, 2000, pp. 35–56.

[8]Hollander, S., "Autonomous Space Robotics: Enabling Technologies for Advanced Space Platforms," AIAA Paper 2000-5079, Sept. 2000.

[9]Purcell, G., Kuang, D., Lichten, S., Wu, S. C., and Young, L., "Autonomous Formation Flyer (AFF) Sensor Technology Development," *21st Annual AAS Guidance and Control Conference*, American Astronautical Society, Breckenridge, CO, 1998, pp. 463–482.

[10]Gilbreath, G. C., Bowman, S. R., Rabinovich, W. S., Merk, C. H., and Senasack, H. E., "Modulating Retroreflector Using Multiple Quantum Well Technology," U. S. Patent 6154299, filed 28 Nov. 2000.

[11]Gilbreath, G. C., Rabinovich, W. S., Meehan, T. J., Vilcheck, M. J., Mahon, R., Burris, R., Ferraro, M., Sokolsky, I., Vasquez, J. A., Bovais, C. S., Cochrell, K., Goins, K. C., Barbehenn, R., Katzer, D. S., Anastasiou, K. I., and Montes, M. J., "Large Aperture Multiple Quantum Well Modulating Retroreflector for Free-Space Optical Data Transfer on Unmanned Aerial Vehicles," *Optical Engineering*, Vol. 40, No. 7, 2001, pp. 1348–1356.

[12]Katzer, D. S., Rabinovich, W. S., Ikossi-Anastasiou, K., and Gilbreath, G. C., "Optimization of Buffer Layers for InGaAs/AlGaAs PIN Optical Modulators Grown on GaAs Substrates by Molecular Beam Epitaxy," *Journal of Vacuum Science Technology B*, Vol. 18, No. 3, 2000, pp. 1609–1613.

[13]Goetz, P. G., Rabinovich, W. S., Walters, R. J., Messenger, S. R., Gilbreath, G. C., Mahon, R., Ferraro, M., Anastasiou, K. I., and Katzer, D. S., "Effects of Proton Irradiation on InGaAs/AlGaAs Multiple Quantum Well Modulators," Inst. of Electrical and Electronics Engineers, Paper 5.0402, March 2001.

[14]Gilbreath, G. C., Rabinovich, W. S., Meehan, T. J., Vilcheck, M. J., Stell, M., Mahon, R., Goetz, P. G., Oh, E., Vasquez, J., Cochrell, K., Lucke, R., and Mozersky, S., "Realtime Video Transfer Using Multiple Quantum Well Retromodulators," *Proceedings of the SPIE*, Vol. 4821, International Society for Optical Engineering, Bellingham, WA, 2002, pp. 155–162.

[15]Rabinovich, W. S., Gilbreath, G. C., Goetz, P. G., Mahon, R., Kazter, D. S., Ikossi-Anasatasiou, K., Binari, S., Meehan, T. J., Ferraro, M., Sokolsky, I., Vasquez, J. A., and Vilcheck, M. J., "InGaAs Multiple Quantum Well Modulating Retroreflector for Free Space Optical Communications," *Proceedings of the SPIE*, Vol. 4489, International Society for Optical Engineering, Bellingham, WA, 2002, pp. 190–201.